Molecular Pharmacology Fast Forward. Published on October 24, 2008 as doi:10.1124/mol.108.050716
This article has not been copyedited and formatted. The final version may differ from this version.

MOL 50716

Phenylephrine-induced cardiomyocyte injury is triggered by superoxide generation through uncoupled eNOS and ameliorated by DY9836, a novel calmodulin antagonist.

Ying-Mei Lu, Feng Han, Norifumi Shioda, Shigeki Moriguchi, Yasufumi Shirasaki, Zheng-Hong Qin, and Kohji Fukunaga*

Department of Pharmacology, Graduate School of Pharmaceutical Sciences, Tohoku University, Sendai, Japan (YML, NS, SM, KF).

Daiichi-Sankyo Pharmaceutical Co., Ltd. Tokyo, Japan (YS).

Institute of Pharmacology & Toxicology and Biochemical Pharmaceutics, College of Pharmaceutical Sciences, Zhejiang University, Hangzhou China (FH)

Department of Pharmacology, Soochow University School of Medicine, Suzhou, China (ZHQ).

Tohoku University 21st Century COE Program “CRESCENDO”, Sendai, Japan (KF)

Molecular Pharmacology Fast Forward. Published on October 24, 2008 as DOI: 10.1124/mol.108.050716
This article has not been copyedited and formatted. The final version may differ from this version.

Running Title: Cardiomyocyte injury is triggered by uncoupled eNOS

Corresponding Author:

Kohji Fukunaga, Ph.D.,
Department of Pharmacology,
Graduate School of Pharmaceutical Sciences, Tohoku University
Aramaki-Aoba Aoba-ku, Sendai 980-8578, Japan
Tel: 81-22-795-6836, Fax: 81-22-795-6835
E-mail: **fukunaga@mail.pharm.tohoku.ac.jp**

Text pages: 36

Words in abstract: 218

Words in introduction: 748

Words in discussion: 1246

References: 48

Figures: 9

Abbreviations: $O_2^{\cdot-}$, superoxide anion; NO , nitric oxide; eNOS, endothelial nitric oxide synthase; nNOS, neuronal nitric oxide synthase; iNOS, inducible nitric oxide synthase; BH_4, tetrahydrobiopterin; SR, sarcoplasmic reticulum; PE, phenylephrine; DMEM, Dulbecco's modified Eagle medium; DAF-FM, 4-amino-5-methylamino-2',7'-difluorofluorescein; DHE, dihydroethidium; TUNEL, TdT-mediated dUTP nick end labeling.

Molecular Pharmacology Fast Forward. Published on October 24, 2008 as DOI: 10.1124/mol.108.050716
This article has not been copyedited and formatted. The final version may differ from this version.

Abstract

The pathophysiological relevance of eNOS-induced superoxide production in cardiomyocyte injury following prolonged PE exposure remains unclear. The aims of this study were to define the mechanism of $O_2^{\cdot-}$ production by uncoupled eNOS and evaluate the therapeutic potential of a novel calmodulin antagonist, DY-9836, {3-[2-[4-(3-chloro-2-methylphenyl)-1-piperazinyl]ethyl]-5,6-dimethoxyindazole}, to rescue hypertrophied cardiomyocytes from PE-induced injury. In cultured rat cardiomyocytes, prolonged exposure for 96h to PE led to translocation from membrane to cytosol of eNOS and breakdown of caveolin-3 and dystrophin. When NO and $O_2^{\cdot-}$ production were monitored in PE-treated cells by DAF-FM and DHE, respectively, Ca^{2+}-induced NO production elevated by 5.7-fold ($p<0.01$) after 48 h PE treatment and the basal NO concentration markedly elevated (16-fold; $p<0.01$) after 96 h PE treatment. On the other hand the $O_2^{\cdot-}$ generation at 96 h was closely associated with an increased uncoupled eNOS level. Co-incubation with DY-9836 (3 μM) during the last 48 h inhibited the aberrant $O_2^{\cdot-}$ generation near completely and NO production by 72% ($P<0.01$) after 96 h of PE treatment and inhibited the breakdown of caveolin-3/dystrophin in cardiomyocytes. PE-induced apoptosis assessed by TUNEL staining was also attenuated by DY-9836 treatment. These results suggest that $O_2^{\cdot-}$ generation by uncoupled eNOS likely triggers PE-induced cardiomyocyte injury. Inhibition of abnormal $O_2^{\cdot-}$ and NO generation by DY-9836 treatment represents an attractive therapeutic strategy for PE/hypertrophy-induced cardiomyocyte injury.

Molecular Pharmacology Fast Forward. Published on October 24, 2008 as DOI: 10.1124/mol.108.050716
This article has not been copyedited and formatted. The final version may differ from this version.

Introduction

NO toxicity is in part mediated by generation of peroxynitrite ($ONOO^-$) with concomitant production of $O_2^{\cdot-}$ under pathological conditions common to heart disease, such as ischemia (Bauersachs et al., 1999) and heart failure (Munzel et al., 1999; Dixon et al., 2003). $ONOO^-$ can trigger lipid peroxidation, protein tyrosine nitration, and DNA strand breakdown (Schulz et al., 1997; Yasmin et al., 1997). The increase in reactive oxygen species, in particular $O_2^{\cdot-}$, is mainly due to activation of plasma membrane NADPH oxidase, mitochondrial respiratory chain enzymes, cyclooxygenase and xanthine oxidase, and causes oxidative stress during heart failure. In addition, uncoupled nitric oxide synthase (NOS) also mediates $O_2^{\cdot-}$ generation in pathological conditions (Vasquez-Vivar et al., 1998; Mollnau et al., 2002). However, the precise mechanism of superoxide production during heart failure remains unclear.

Among three NOS isoforms (neuronal, inducible and endothelial), eNOS is easily uncoupled under conditions of cofactor BH_4 depletion, in which dissociation of eNOS dimer also promotes $O_2^{\cdot-}$ generation (Forstermann et al., 2006). In the absence of BH_4, eNOS generates $O_2^{\cdot-}$ from breakdown of the heme-dioxygen complex at the oxygenase domain of the enzyme (Fig. 8), while electron flow from the reductase to the oxygenase domain is diverted to molecular oxygen rather than to L-arginine (Verhaar et al. 2004). $O_2^{\cdot-}$ generation by uncoupled eNOS cannot be prevented by supplementary L-arginine (Xia et al. 1998). By contrast, nNOS and iNOS isoforms are relatively difficult to uncouple, even in the absence of cofactors. $O_2^{\cdot-}$ generation by nNOS and iNOS is minimally induced by L-arginine depletion (Pou et al., 1992; Xia et al., 1996). Thus, eNOS uncoupling accompanied by BH_4 depletion is thought to be crucial for heart damage following cardiovascular disorders, including hypertension (Forstermann et al.,

Molecular Pharmacology Fast Forward. Published on October 24, 2008 as DOI: 10.1124/mol.108.050716
This article has not been copyedited and formatted. The final version may differ from this version.

2006), atherosclerosis (Lahera et al., 2007), diabetes (Thum et al., 2007). Furthermore, eNOS uncoupling has been documented in mice subjected to sustained pressure overload, thereby resulting in increased $O_2^{\cdot-}$ production with concomitant disruption of the eNOS dimer (Takimoto et al., 2005). Likewise, oxidative stress in an experimental model of idiopathic dilated cardiomyopathy is mediated by uncoupled eNOS through activation of the renin-angiotensin systems **(**Mollnau et al., 2005).

In cardiac myocytes the eNOS isoform mostly localizes to caveolae, where it associates with caveolin-3 (Garcia-Cardena et al., 1996; Feron et al., 1996). Unlike eNOS, nNOS localize primarily to SR (Xu et al., 1999). In resting conditions, binding to caveolin-3 inhibits eNOS activity, thereby limiting NO production, whereas calmodulin binding to eNOS disrupts caveolin-3 binding, leading to eNOS activation (Michel et al., 1997). Moreover, in cardiomyocytes G-protein-coupled α1-adrenergic receptors are enriched in caveolae and colocalize with caveolin-3 (Fujita et al., 2001). Stimulation of α1-adrenergic receptors with PE upregulates caveolin-3 in cardiomyocytes (Kikuchi et al., 2005). Indeed, following PE stimulation, eNOS dissociates from caveolin-3 and translocates to the cytosol (Michel et al., 1997). Molnar et al. (2005) reported that pathological interference with eNOS dimerization impairs NO-dependent endothelial function, without changing eNOS phosphorylation status. However, the physiological relevance of caveolin-3 and calmodulin to eNOS uncoupling upon PE-stimulation remains unclear.

Our previous studies demonstrated that exposure of cardiomyocytes to angiotensin II, endothelin-1 or PE markedly increased cell size after 48 h of treatment with these reagents, most likely representing compensatory hypertrophy. More prolonged exposure to these factors, disrupts Ca^{2+} regulation by the sarcoplasmic reticulum, causing

Molecular Pharmacology Fast Forward. Published on October 24, 2008 as DOI: 10.1124/mol.108.050716
This article has not been copyedited and formatted. The final version may differ from this version.

cardiomyocyte dysfunction including caveolin-3/dystrophin breakdown (Lu et al., 2007). These in vitro models allowed us to test the effects of novel cardioprotective drugs on caveolin-3/dystrophin breakdown in humoral factor-induced cardiac injury. We previously showed that DY-9760e, a novel calmodulin antagonist, inhibited nNOS and eNOS and reduced NO production in N1E-115 cells (Fukunaga et al., 2000). However, DY-9760e also inhibits cytochrome P450 enzymes in the liver. Thus clinically achievable efficacy is limited by predicted drug interaction by DY-9760e in drug metabolism in humans (Tachibana et al., 2005). Importantly, we showed that DY-9836, as an N-de-alkylated DY-9760e and active metabolite, produced cardioprotective effects against cardiac hypertrophy induced by endothelin-1 and angiotensin II (Lu et al., 2007). Unlike DY-9760e, DY-9836 does not interfere with metabolism of other drugs in the liver (Tachibana et al., 2005), suggesting that it is more attractive candidate than DY-9760e for clinical therapy.

To understand precise mechanisms of oxidative cardiomyocyte injury induced by humoral factors causing hypertrophy, we first focused on spatiotemporal changes in eNOS and caveolin-3 expression during prolonged exposure to PE and determined whether eNOS accounts for both NO and $O_2^{\cdot -}$ production in the pathological conditions. We also address whether inhibiting uncoupling of eNOS by a novel CaM inhibitor, DY-9836, ameliorates PE-induced cardiomyocyte injury.

Molecular Pharmacology Fast Forward. Published on October 24, 2008 as DOI: 10.1124/mol.108.050716
This article has not been copyedited and formatted. The final version may differ from this version.

Materials and Methods

Cell culture. Neonatal ventricular myocytes were isolated from hearts of 1- to 3-day-old Wistar rats by collagenase digestion and cultured according to the method of Waspe et al (1990). Briefly, myocytes were dissociated from ventricles by serial digestion with 0.1% trypsin and 0.05% DNase I in Hank's balanced salt solution. After each digestion, digested cardiomyocytes were collected and suspended in DMEM with 10% fetal bovine serum (FBS) and 0.02 % trypsin inhibitor to block further trypsin digestion. Cells were collected by centrifugation (4 °C, 1,000 × g for 10 min). After the supernatant was removed, DMEM containing 10% FBS was added. Cells were gently agitated and plated on uncoated 90-mm culture dishes. Plates were allowed to stand for 30 min in a CO_2 incubator at 37°C to remove nonmyocytes attached to the culture plates. Unattached myocytes were collected and plated at 1-2 × 10^6 cells per 35-mm dish and incubated with DMEM and 10 % FBS in a humidified incubator with 5% CO_2 at 37°C for 24 h. Cells were cultured in serum-free DMEM for 24 h before treatment with PE (10 μM).

Membrane fractionation. Membrane fractionation from cultured cardiomyocytes was performed as described (Ostrom et al., 2001). Briefly, cells were homogenized in buffer containing 500 mM sodium carbonate plus 50 μg/ml leupeptin, 25 g/ml pepstatin A, 100 nM calyculin A, 50 g/ml trypsin inhibitor and 1 mM dithiothreitol. The homogenate was adjusted to 45% sucrose by adding 90% sucrose in 25 mM MES, 150 mM NaCl, pH 6.5, and loaded in an ultracentrifuge tube. A discontinuous sucrose gradient was layered on top of the sample by placing 4 ml of 35% sucrose and then 4 ml

Molecular Pharmacology Fast Forward. Published on October 24, 2008 as DOI: 10.1124/mol.108.050716
This article has not been copyedited and formatted. The final version may differ from this version.

of 5% sucrose. The gradient was centrifuged at 39,000 rpm on a SW41Ti rotor (Beckman Instruments) for 16 h at 4 °C. Fractions were collected in 1-ml aliquots from the top of the gradient.

Western blot analysis. Cultured cells were washed with cold PBS and stored at -80 °C until immunoblotting analyses were performed as described (Lu et al. 2007). Briefly, equal amounts of proteins were separated on 7.5-10% SDS-PAGE gels and transferred to a PVDF membrane (Millipore Corporation, Bedford, MA, U.S.A.). Blots were stained with 0.1% Ponceau S solution to visualize protein bands and confirm equal protein loading. After blocking in 5% non-fat milk, blots were incubated overnight at 4°C with antibodies against anti-eNOS and iNOS (Sigma, St. Louis, MO) (rabbit polyclonal antibody diluted 1:200), caveolin-3 and dystrophin (Chemicon International, Temecula, CA) (mouse monoclonal antibodies diluted 1:1000), monoclonal anti-nitrotyrosine antibody (1:500, Upstate Biotechnology, Lake Placid, NY, U.S.A.) For immunoblot analysis of dimeric eNOS, samples were not heated and gel temperature was maintained below 15°C during electrophoresis (low-temperature SDS-PAGE) as described (Zou et al., 2002). Immunoreactive proteins on the membrane were visualized with an enhanced chemiluminescence detection system (Amersham Life Science, Buckinghamshire, UK). Images were scanned and analyzed semiquantitatively using NIH Image and Image Gauge Software (Fujifilm, Tokyo, Japan).

Measurement of intracellular NO production. Intracellular NO was fluorometrically assessed with the NO-sensitive fluorescence probe DAF-FM (Kojima et al., 1998).

Molecular Pharmacology Fast Forward. Published on October 24, 2008 as DOI: 10.1124/mol.108.050716
This article has not been copyedited and formatted. The final version may differ from this version.

Briefly, cells were loaded with 10 μM DAF-FM diacetate, a cell-permeant form of DAF-FM, at 37°C for 30 min in Tyrode buffer containing 150 mM NaCl, 4 mM KCl, 1 mM $MgCl_2$, 2 mM $CaCl_2$, 5.6 mM glucose, and 5 mM HEPES (pH 7.4). After loading, cells were rinsed three times with Tyrode buffer and then placed on the stage of a Leica inverted microscope equipped with an epifluorescence attachment. During the experiments, cells were superfused in a 0.3-ml bath chamber at 37°C under a constant flow (1 ml/min) of Tyrode buffer containing L-arginine (1 mM). NO fluorescence from each well was measured at excitation and emission wavelengths of 488 nm and 520 nm, respectively. Background fluorescence was measured and subtracted from each reading.

Measurement of intracellular superoxide production. Superoxide production in cultured cardiomyocytes was assayed using the oxidative fluorescent dye DHE. DHE is oxidized on reaction with $O_2^{\cdot-}$ to ethidium bromide with fluorescence (Benov et al., 1998). For in vitro studies, equal numbers of cultured cardiomyocytes in 35-mm plates were incubated in serum-free medium with or without L-NAME (100 μM), apocynin (10 μM) and TEMPOL (1 mM), in the presence or absence of PE and DY-9836 for 48h or 96h. After 48 h or 96 h treatments, the fresh culture medium with HE (10 mM, Molecular Probes) was added to cells. Then after a 30-min incubation period during which DHE was oxidized to the fluorophore ethidium, cells were washed with 37ºC PBS and maintained in 1-ml of culture medium, and then placed on the inverted microscope stage. DHE conversion to ethidium (Eth) was used to determine intracellular $O_2^{\cdot-}$ levels, and signals were collected through a 590 nm filter after excitation of cells at 488 nm. Images were collected by fluorescence microscopy and equal numbers of cells (10 cells from each field, five fields total) were analyzed using

Molecular Pharmacology Fast Forward. Published on October 24, 2008 as DOI: 10.1124/mol.108.050716
This article has not been copyedited and formatted. The final version may differ from this version.

the Metamorph Image System (Molecular Devices Corp., Downingtown, PA). Background fluorescence was measured simultaneously to confirm that responses were specific to intracellular $O_2^{\cdot-}$.

TUNEL assay. Double-staining using TUNEL for apoptotic cell nuclei and propidium iodide (PI) for myocardial cell nuclei was undertaken. TUNEL staining was performed using a Takara in situ apoptosis detection kit (Takara. Bio Inc., Shiga, Japan), according to the manufacturer's protocol. Cardiomyocytes from at least four randomly selected slides per block were evaluated immunohistochemically to determine the number and percentage of cells exhibiting staining indicative of apoptosis. For each slide, 10 fields were randomly chosen, and 100 cells per field were counted using a defined rectangular field area (20 × objective). The index of apoptosis (number of apoptotic myocytes/the total number of myocytes counted x 100%) was determined from 60 fields per slide.

Morphological alteration of cardiomyocytes. Morphological changes in cultured myocytes were examined using rhodamine-phalloidin (1:300; Molecular Probes, Eugene, OR) as described (Lu et al. 2007). Briefly, after incubation with phenylephrine for 48 or 96 h in the presence or absence of DY-9836 (3 μM), TEMPOL (1mM) and L-NAME (100 μM), cultured cells were washed 3 times in PBS and fixed in 4% formaldehyde. After permeabilization with 0.1% Triton X-100 in PBS, fixed cells were incubated with 1% bovine serum albumin in PBS for 30 min. Cells were incubated for 3 h at room temperature with rhodamine-phalloidin in PBS containing 1% bovine serum albumin. Images were captured with a CCD camera (Olympus).

Molecular Pharmacology Fast Forward. Published on October 24, 2008 as DOI: 10.1124/mol.108.050716
This article has not been copyedited and formatted. The final version may differ from this version.

Immunocytochemistry. Immunolocalization and changes of caveolin-3, eNOS and dystrophin in cultured myocytes were examined by immunocytochemistry. Briefly, after incubation in the presence or absence of phenylephrine with DY-9836 (3 μM) for 48 or 96 h, cultured cells were washed 3 times in PBS and fixed in 4% formaldehyde. For immunolabeling, fixed cells were incubated with anti-caveolin-3 (mouse monoclonal antibody; 1:200, Upstate Biotechnology, Lake Placid, NY) or dystrophin (mouse monoclonal antibody; 1:1000, Chemicon, Temecula, CA), with anti-eNOS (rabbit polyclonal antibody; 1:200) overnight at 4°C. After washing, sections were incubated with biotinylated anti-rabbit IgG (1:5000) in TNB buffer for 1 hour, followed by both streptavidin-HRP (1:5000) and Alexa 594 anti mouse IgG (Molecular Probes, Eugene, OR, USA) in TNB buffer (1:400) and labeled for 2 hours. Sections were then stained with tetramethylrhodamine tyramide for 10 minutes using the TSA-Detect kit (NEN Life Science Products, Boston, MA). Immunofluorescent images were taken with a confocal laser scanning microscope (TCS SP, Leica Microsystems).

Statistical analyses. All values are expressed as means ± S.E.M. Multiple comparisons between experimental groups were made by ANOVA followed by Dunnett's test. $P<0.05$ was considered significant.

Molecular Pharmacology Fast Forward. Published on October 24, 2008 as DOI: 10.1124/mol.108.050716
This article has not been copyedited and formatted. The final version may differ from this version.

Results

Temporal changes in caveolin-3 and eNOS in cardiomyocyte membrane fractions following prolonged exposure to PE. Prolonged exposure to PE dissociates eNOS from caveolae to the soluble subcellular compartment (Michel et al., 1993). We first measured levels of eNOS and caveolin-3 in both membrane and cytosol fractions of cardiomyocytes after prolonged exposure to PE. Membrane and cytosol extracts were prepared from cardiomyocytes cultured from 24 to 96 h in PE (10 μM). Interestingly, in the membrane fraction both eNOS and caveolin-3 levels significantly increased up to the 48 h time point, followed by a decrease up to 96 h (Fig.1A; 1B). To address whether these changes were due to protein translocation, cytosolic and membrane levels of both eNOS and caveolin-3 were quantified. In the case of eNOS, increased levels seen in the membrane fraction contrasted with decreased levels seen in the cytosol, suggestive of translocation (Fig.1A; 1B). Unchanged total eNOS levels seen in total homogenates confirmed eNOS translocation. By contrast, increased caveolin-3 levels in the membrane fraction were attributable to increased expression of total caveolin-3 up until the 48 h time point. Since total caveolin-3 levels significantly decreased by 96 h of PE exposure, the reduction of caveolin-3 observed at 72-96 h is apparently due to its breakdown.

Change in NO production following prolonged PE treatment. Since the eNOS level was dramatically and biphasically changed between 48 and 96 h of PE treatment, we characterized basal and A23187-induced NO production at 48 and 96 h using DAF-FM. Without PE treatment, basal DAF fluorescence intensity was less than the arbitrary unit

Molecular Pharmacology Fast Forward. Published on October 24, 2008 as DOI: 10.1124/mol.108.050716
This article has not been copyedited and formatted. The final version may differ from this version.

20. When calcium ionophore A23187 was applied to the incubation chamber, a faint and transient increase in the DAF signal was observed. Consistent with increased eNOS levels seen at 48 h in the membrane fraction, basal DAF fluorescence slightly but significantly increased 1.4-fold (Fig 2A-b). Interestingly, A23187 treatment dramatically and persistently increased NO production at 48 h of PE treatment. To confirm that marked NO increase was due to increased membrane eNOS, we added a novel calmodulin inhibitor, DY-9836, to the incubation chamber before A23187 application. DY-9836 dose-dependently inhibited both basal and A23187-induced NO production (Fig 2A-c). More importantly, basal DAF fluorescence dramatically increased up to an arbitrary unit of 400 in cells exposed to PE for 96 h, and A23187 application failed to stimulate NO production. These results strongly suggested that translocation of eNOS into the membrane fraction accounts for aberrant NO production after 48 h of prolonged exposure to PE and that DY-9836 potently inhibited Ca^{2+}/CaM-dependent eNOS in cultured cardiomyocytes.

NO production with or without PE treatment is summarized in Fig. 2B. Prolonged exposure to PE for 96 h increased NO levels 16 -fold (Fig 2B). A23187 application did not stimulate NO production further at 96 h, suggesting that aberrant and persistent NO production masks Ca^{2+}-dependent NO production by eNOS and that Ca^{2+}-independent NOS is also involved in persistent NO production at 96 h. Indeed, an increase in iNOS protein after 72-96 h of PE exposure was observed in cultured cardiomyocytes (Supplementary Fig.1A). Co-incubation with DY-9836 during the last 48 h partly but significantly inhibited iNOS production by 32% as compare to PE 96 h group (Supplementary Fig.1A).

Molecular Pharmacology Fast Forward. Published on October 24, 2008 as DOI: 10.1124/mol.108.050716
This article has not been copyedited and formatted. The final version may differ from this version.

Change in superoxide production following prolonged PE treatment. To verify involvement of eNOS in superoxide production after prolonged PE treatment, we measured intracellular superoxide production by DHE fluorescence with or without PE treatment at 48 h and 96 h. Basal DHE fluorescence intensity was approximately 300 as an arbitrary unit. Since basal DHE fluorescence was not affected by treatment with apocynin, a NADPH oxidase inhibitor, it is likely due to autofluorescence of cells or the culture dish. Basal DHE fluorescence was not also affected by A23187 and L-NAME treatment in control cells without PE treatment, suggesting that the superoxide production in control cells is insensitive to Ca^{2+} elevation and eNOS activity (Fig. 3A-a). PE treatment for 48 h slightly but significantly increased basal superoxide production due to NADPH oxidase activity, which was inhibited by apocynin treatment. Interestingly, A23187 application inhibited superoxide production (Fig. 3A-b). A23187-induced inhibition of superoxide production was restored by L-NAME application, suggesting that A23187-induced NO production by eNOS quenches superoxide produced by PE treatment at 48 h. More importantly, a marked increase in the basal superoxide production was observed at 96 h of PE treatment (Fig 3A-c). The superoxide production at 96 h was largely inhibited by apocynin treatment, suggesting involvement of NADPH oxidase in superoxide generation at 96 h. At 96 h, A23187 application did not quench superoxide, but L-NAME substantially inhibited aberrant production of superoxide, suggesting that, in addition to NADPH oxidase, eNOS is partly responsible for superoxide production at 96 h. Consistent with our hypothesis, acute DY-9836 treatment dose-dependently inhibited superoxide production at 96 h (Fig 3A-d; 3B-c).

Molecular Pharmacology Fast Forward. Published on October 24, 2008 as DOI: 10.1124/mol.108.050716
This article has not been copyedited and formatted. The final version may differ from this version.

To define mechanisms underlying increases in superoxide production after prolonged PE exposure, we measured levels of dimeric and monomeric forms of eNOS at 48 and 96 h using low-temperature SDS-PAGE (Fig. 3C). As shown in Fig. 3C, the ratio of dimeric to monomeric eNOS in control cardiomyocytes without PE treatment was defined. That ratio was elevated 1.5 fold ($p<0.05$) at 48 h compared to the control group, whereas at 96 h it fell 0.5 fold. We also assessed the ratio of dimeric/monomeric eNOS in the membrane fraction. Consistent with the observation with total extracts (Fig. 3C), the ratio increased by 67% at 48 h and decreased by 40% at 96 h compare to the control (supplementary Fig.2). Taken together, the present observation suggests that uncoupled and monomeric eNOS accounts for superoxide production following prolonged PE exposure.

Effect of prolonged DY-9836 treatment on PE-induced intracellular NO and O_2^- generation. Since acute DY-9836 treatment of cardiomyocytes effectively inhibited both NO production and superoxide production at 48 and 96 h of PE treatment, we confirmed whether prolonged DY-9836 treatment inhibits NO and superoxide production. DY-9836 (1 and 3μM) with or without L-NAME (100 μM) or the superoxide scavenger Tempol (1 mM) was added at 48 h in culture medium after PE treatment. Increased NO production seen at 96 h was dose-dependently inhibited by 26% and 72% by 1 and 3 μM DY-9836, respectively (Fig. 4A). L-NAME (100 μM) treatment completely inhibited NO production, suggesting that NO production is due to nitric oxide synthase activation at 96 h (Fig. 4A).

DY-9836 treatment also inhibited PE-induced superoxide production at 96 h. Treatment with 1 and 3 μM DY-9836 reduced superoxide production by 27 and 56%,

Molecular Pharmacology Fast Forward. Published on October 24, 2008 as DOI: 10.1124/mol.108.050716
This article has not been copyedited and formatted. The final version may differ from this version.

respectively (Fig. 4B). Moreover, Tempol (1mM) completely scavenged superoxide generated by PE treatment and L-NAME (100 μM) decreased PE-induced superoxide production by 34% (Fig. 4B).

Furthermore, we investigated changes of protein tyrosine nitration, which reflects formation of peroxynitrate ($ONOO^-$). Western blotting with anti-nitrotyrosine antibody revealed that protein tyrosine nitration of a 45kDa protein was significantly increased by 177% and DY-9836 (3 μM) treatment completely inhibited the increase (Supplementary Figure 3).

Effect of DY-9836 on cleavage of dystrophin and cav-3, and on expression of eNOS. We previously documented that prolonged endhotelin-1 treatment induced upregulation of dystrophin at 48 h and breakdown of dystrophin at 96 h by calpain activation (Lu et al. 2007). Here we confirmed that dystrophin was upregulated at 48 h and cleaved at 96 h (Fig. 5A). As shown previously, dystrophin breakdown at 96 h was significantly inhibited by DY-9836 treatment. A similar result also observed in a immunocytochemical experiment (Supplementary Fig. 4). Strong immunoreactivity for dystrophin was restored by the DY-9836 treatment. We also found that DY-9836 treatment completely rescues caveolin-3 breakdown at 96 h dose-dependently (Fig. 5B). Furthermore, DY-9836 treatment significantly restored the eNOS dimer:monomer ratio dose-dependently, suggesting that DY-9836 treatment protects eNOS dimer from disruption (Fig. 5C).

DY-9836 treatment of cardiomyocytes inhibits PE-induced apoptosis. Prolonged activation of the Gq-coupled receptor by PE leads to cardiomyocyte apoptosis in

Molecular Pharmacology Fast Forward. Published on October 24, 2008 as DOI: 10.1124/mol.108.050716
This article has not been copyedited and formatted. The final version may differ from this version.

cultured cardiomyocytes (Adams et al., 2000). Here we also examined a potential effect of DY-9836 on PE-induced apoptosis. As showed in figure 6B, the number of TUNEL-positive nuclei increased by 7% and 37% of control values at 48 h and 96 h, respectively, of PE stimulation. DY-9836 (3 μM) treatment significantly blocked apoptosis to control levels. Likewise, treatment with TEMPOL (1mM) and L-NAME (100 μM) almost completely inhibited the PE-induced apoptosis at 96 h (Fig. 6B). The data suggest that inhibition of eNOS activity and superoxide generation inhibits PE-induced myocardial apoptotic cell death.

Effect of DY-9836 treatment on morphology of cardiomyocytes. We next asked whether PE exposure induces morphological changes in cultured rat cardiomyocytes and, if so, whether DY-9836 could rescue these phenotypes. Cells were stained with rhodamine-phalloidin to label actin filaments and immunostained by anti-caveolin-3 and anti-eNOS antibodies (Fig. 7). Rhodamine-phalloidin fluorescence of PE-treated cells showed a marked increase in the cell surface areas at 48 and 96 h, suggesting cardiomyocyte hypertrophy (Fig. 7B). PE-induced enlargement of the cell area was attenuated by treatment with DY-9836 but not by TEMPOL (1mM) and L-NAME (100 μM) (Fig. 7C). Notably, PE treatment for 48 h increased caveolin-3 and eNOS immunofluorescence. eNOS immunofluorescence was more intense in stress fiber-like structures. Notably, this eNOS immunofluorescence decreased in the membrane fraction 96 h after PE exposure and partly rescued by DY-9836 treatment (3μM) (Fig. 7A). Taken together with results shown in Fig. 8, DY-9836 likely exerts a cardioprotective effect not only by inhibiting eNOS translocation but also by inhibiting hypertrophy.

Molecular Pharmacology Fast Forward. Published on October 24, 2008 as DOI: 10.1124/mol.108.050716
This article has not been copyedited and formatted. The final version may differ from this version.

Discussion

Here we addressed the pathophysiological relevance of eNOS-induced superoxide production following prolonged Gq-coupled receptor stimulation in cultured cardiomyocytes. Our results provide the following novel evidence for PE-induced changes in cardiomyocytes. 1) eNOS translocation from the cytosol to the membrane fraction reinforces the idea that NO production is accompanied by increased cell size and elevated caveolae components, including eNOS, caveolin-3 and dystrophin. 2) Prolonged humoral stress by PE exposure triggers breakdown of caveolin-3 and dystrophin, disrupting caveolae structure. 3) Disrupted caveolae structure synergistically leads to eNOS release from caveolae and in turn promotes eNOS uncoupling. 4) Uncoupled eNOS accounts for the large increase in superoxide generation, inducing oxidative stress and apoptosis. 5) Finally, we provide strong evidence that DY-9836, a novel calmodulin inhibitor, inhibits not only abnormal NO generation by coupled eNOS but also detrimental superoxide generation by uncoupled eNOS (Fig.9).

Accumulating evidence shows that eNOS uncoupling underlies oxidative injury in the setting of cardiovascular risk factors. We found that increased eNOS monomer was significantly induced after 96 h of PE-stimulation. Dixon et al. suggested that NOS monomer produces superoxide anion, whereas the NOS dimer produces NO in the presence of the substrate L-arginine and cofactors such as BH_4 (Fig.8). The marked increased in superoxide was also accelerated by oxidation of BH_4 to BH_2. Reduced BH_4 with uncoupling of eNOS further augments superoxide generation, inducing cardiomyocyte injury. Although our data indicate the importance of eNOS uncoupling in PE-induced $O_2^{\cdot-}$ generation in cardiomyocytes, other pathways could also contribute

Molecular Pharmacology Fast Forward. Published on October 24, 2008 as DOI: 10.1124/mol.108.050716
This article has not been copyedited and formatted. The final version may differ from this version.

to this response. NADPH oxidase subunits are expressed in cardiomyocytes (Xiao et al., 2002) and associated with decreased cell viability in cultured neonatal ventricular myocytes (Kurdi et al., 2007). We used apocynin to investigate the role of NADPH oxidase in PE-induced cardiomyocyte injury. Consistent with previous reports (Qin et al., 2006), our results indicate that apocynin markedly decreased PE-induced superoxide generation at 96 h. Therefore, our data demonstrate that a simultaneous increase in NADPH oxidase and uncoupled eNOS activities largely accounts for PE-induced toxic superoxide production.

We also showed here that not only NO production but also superoxide generation are dependent on Ca^{2+}/calmodulin activation. Consistent with our previous study using DY-9760e (Fukunaga et al. 2000; Hashiguchi et al. 2003), Ca^{2+}-induced NO generation by eNOS was almost completely inhibited by DY-9836. Likewise, DY-9836 significantly attenuated superoxide production at 96 h of PE treatment. The partial inhibition is likely due to increased NADPH oxidase activity in hypertrophic cardiomyocytes, as shown in Fig. 3B. Importantly, stronger inhibition by DY-9836 was seen as PE exposure time increased from 48 to 96 h, as seen in Fig. 4B.

Like nNOS and iNOS, eNOS consists of a C-terminal reductase domain exhibiting binding sites for FAD, FMN and NADPH; an intervening CaM-binding domain; and an N-terminal P450-like oxygenase heme domain with binding sites for iron protoporphyrin IX (hem), BH_4 and L-Arg (Ghosh and Stuehr, 1995). Electrons are transported by NADPH to the reductase domain and processed via FAD and FMN redox carriers to the oxygenase domain. Notably, electron flow through the reductase domain requires bound Ca^{2+}/CaM (Ghosh and Stuehr, 1995). BH_4 and eNOS dimerization are required for electron flow from the reductase domain to the heme of the oxygenase

domain (Fig.8). Under normal physiological conditions, eNOS dimerizes, and electrons transfer from NADPH to heme in the oxygenase domain through FAD and FMN in the reductase domain. In turn, the substrate L-Arg is oxidized in the oxygenase domain to L-citrulline and NO. Thus, in the present study, lack of BH4 by oxidative stress and/or disruption of dimerization occurring in pathological conditions likely induce generation of toxic radicals such as superoxide by eNOS (Stuehr et al., 2001).

Superoxide generation by the reductase domain is activated by Ca^{2+}/CaM in nNOS (Craig et al., 2002). Likewise, electron transfer in the reductase domain is also CaM-sensitive in human endothelial NOS (Nishino et al., 2007). Therefore, we hypothesized that the CaM antagonist, DY-9836, would prevent superoxide generation as well as NO generation during prolonged PE treatment. Consistent with our hypothesis, aberrant NO elevation at 96 h was blocked by prolonged incubation with DY-9836. Likewise, aberrant superoxide production was also largely attenuated by DY-9836 treatment. The inhibitory dose of DY-9836 for both NO and superoxide generation was similar, suggesting that CaM sensitivity is almost equivalent in both coupled and uncoupled eNOS. These observations are potentially important because uncoupled eNOS generates superoxide.

L-NAME and Tempol totally inhibited the NO and superoxide generation, respectively, at 96 h after PE exposure (Fig. 4). We addressed a question whether NO and superoxide mediate cardiomyocyte apoptosis and hypertrophy. Interestingly, the treatment with L-NAME or Tempol totally inhibited the apoptosis after prolonged PE exposure (Fig. 6), whereas failed to inhibit cardiomyocyte hypertrophy (Fig 7). Thus No and superoxide likely trigger the PE-induced apoptosis but not mediate PE-induced cardiomyocyte hypertrophy. The inhibition both of apoptosis and hypertrophy by

DY-9836 suggests its diverse actions to protect cardiomyocytes from oxidative and hypertrophic injuries.

The eNOS-derived superoxide has been shown to be associated with development and progression of atherosclerosis and hypertension (Cosentino et al.,1998; Ozaki et al., 2002).Under physiological conditions, eNOS is localized to caveolae through caveolin-3 in cardiomyocytes. Binding of CaM to eNOS promotes dissociation of eNOS from caveolin-3 concomitant with activation. Since the cardiac muscle fibers of caveolin-3 knockout mice showed loss of caveolae and impaired excitation-contraction coupling, thereby leading to cardiac hypertrophy (Woodman et al., 2002), translocation of caveolin-3 from the membrane to the cytosol seen at 96 h likely accelerates disruption of caveolae. In addition, caveolae structure is essential for coupling between voltage-dependent Ca^{2+} channels and intracellular Ca^{2+} channels such as the ryanodine receptor in sarcoplasmic reticulum (Scriven et al., 2005). Thus caveolin-3 breakdown may impair intracellular Ca^{2+} mobilization by excitation-contraction coupling in cardiomyocytes after prolonged PE treatment. Indeed we previously observed impaired caffeine-induced Ca^{2+} mobilization at 96 h under the same conditions (Lu et al., 2007). Although precise mechanisms of eNOS translocation and uncoupling remain unclear, perturbed caveolae structure following caveolin-3 breakdown also promotes eNOS translocation. The eNOS phosphorylation at Thr496 by protein kinase C and at Ser1177 by protein kinase B and Ca^{2+}/CaM-dependent protein kinase II also regulates eNOS activity (Mount et al., 2007). Therefore, further extensive studies are required to understand the pathological relevance of these phosphorylation steps in aberrant NO and superoxide production in PE-induced injury.

We also found that dystrophin breakdown precedes caveolin-3 dissociation from the

Molecular Pharmacology Fast Forward. Published on October 24, 2008 as DOI: 10.1124/mol.108.050716
This article has not been copyedited and formatted. The final version may differ from this version.

plasma membrane (Supplementary Fig. 1B). Since caveolin-3 binds directly to the dystrophin-glycoprotein complex through the PPXY motif in the C-terminal tail of α-dystroglycan (Sotgia et al., 2000), dystrophin breakdown may trigger translocation of caveolin-3 from caveolae. In addition, we previously documented that DY-9836 inhibits dystrophin breakdown in cultured cardiomyocytes (Lu et al., 2007). Therefore, we propose that the cardioprotective effects of DY-9836 partly due to inhibition of dystrophin breakdown, as previously proposed (Lu et al., 2007).

In conclusion, we demonstrate that superoxide generation resulting from uncoupling of eNOS accounts for PE-induced cardiomyocyte injury. Dissociation of caveolin-3 and dystrophin from the plasma membrane leads to eNOS uncoupling. Breakdown of caveolin-3 and dystrophin was also elicited by calpain activation as previously described (Lu et al., 2007). Both inhibition of superoxide generation and breakdown of caveolin-3 and dystrophin by DY-9836 likely mediate its cardiomyocyte protective effects in hypertrophied cardiomyocytes (Fig. 9). These mechanisms provide a novel therapeutic intervention for cardiac hypertrophy and heart failure. In this context, we strongly suggest the effectiveness of DY-9836 treatment on progression of cardiac pathology in vivo, including cardiac dysfunction, injury, and mortality associated with heart failure.

References:

Adams JW, Pagel AL, Means CK, Oksenberg D, Armstrong RC and Brown JH (2000) Cardiomyocyte apoptosis induced by Galphaq signaling is mediated by permeability transition pore formation and activation of the mitochondrial death pathway. *Circ Res* **87:**1180-1187.

Bauersachs J, Bouloumié A, Fraccarollo D, Hu K, Busse R and Ertl G (1999) Endothelial dysfunction in chronic myocardial infarction despite increased vascular endothelial nitric oxide synthase and soluble guanylate cyclase expression: role of enhanced vascular superoxide production. *Circulation* **100:**292-298.

Benov L, Sztejnberg L and Fridovich I (1998) Critical evaluation of the use of hydroethidine as a measure of superoxide anion radical. *Free Radic Biol Med* **25:**826-831.

Cosentino F, Patton S, d'Uscio LV, Werner ER, Werner-Felmayer G, Moreau P, Malinski T and Lüscher TF (1998) Tetrahydrobiopterin alters superoxide and nitric oxide release in prehypertensive rats. *J Clin Invest* **101:**1530-1537.

Craig DH, Chapman SK and Daff S (2002) Calmodulin activates electron transfer through neuronal nitric-oxide synthase reductase domain by releasing an NADPH-dependent conformational lock. *J Biol Chem* **277:**33987-33994.

Dixon LJ, Morgan DR, Hughes SM, McGrath LT, El-Sherbeeny NA and Plumb RD (2003) et al. Functional consequences of endothelial nitric oxide synthase uncoupling in congestive cardiac failure. *Circulation* **107:**1725-1728.

Feron O, Belhassen L, Kobzik L, Smith TW, Kelly RA and Michel T (1996) Endothelial nitric oxide synthase targeting to caveolae. Specific interactions with caveolin isoforms in cardiac myocytes and endothelial cells. *J Biol Chem* **271:**22810-22814.

Förstermann U, Münzel T (2006) Endothelial nitric oxide synthase in vascular disease: from marvel to menace. *Circulation* **113:**1708-1714.

Fujita T, Toya Y, Iwatsubo K, Onda T, Kimura K, Umemura S and Ishikawa Y (2001) Accumulation of molecules involved in alpha1-adrenergic signal within caveolae: caveolin expression and the development of cardiac hypertrophy. *Cardiovasc Res* **51:**709-716.

Fujita T, Toya Y, Iwatsubo K, Onda T, Kimura K, Umemura S and Ishikawa Y (2000) Inhibition of neuronal nitric oxide synthase activity by 3-[2-[4-(3-chloro-2-methylphenyl)- 1-piperazinyl]ethyl]-5, 6-dimethoxy-1-(4-imidazolylmethyl)-1H-indazole dihydrochloride 3.5 hydrate (DY-9760e), a novel neuroprotective agent, in vitro and in cultured neuroblastoma cells in situ. *Biochem Pharmacol* **60:**693-699.

Garcia-Cardena G, Oh P, Liu J, Schnitzer JE and Sessa WC (1996) Targeting of nitric oxide synthase to endothelial cell caveolae via palmitoylation: implications for nitric oxide signaling. *Proc Natl Acad Sci U S A* **93:**6448-6453.

Ghosh DK and Stuehr DJ (1995) Macrophage NO synthase: characterization of isolated oxygenase and reductase domains reveals a head-to-head subunit interaction. *Biochemistry* **34:**801-807.

Hashiguchi A, Kawano T, Yano S, Morioka M, Hamada J, Sato T, Shirasaki Y, Ushio Y and Fukunaga K (2003) The neuroprotective effect of a novel calmodulin antagonist, 3-[2-[4-(3-chloro-2-methylphenyl)-1-piperazinyl]ethyl]-5,6-dimethoxy-1-(4-imidaz olylmethyl)-1H-indazole dihydrochloride 3.5 hydrate, in transient forebrain ischemia. *Neuroscience* **121:**379-386.

Kikuchi T, Oka N, Koga A, Miyazaki H, Ohmura H and Imaizumi T (2005) Behavior of

caveolae and caveolin-3 during the development of myocyte hypertrophy. *J Cardiovasc Pharmacol* **45:**204-210.

Kojima H, Nakatsubo N, Kikuchi K, Kawahara S, Kirino Y, Nagoshi H, Hirata Y and Nagano T (1998) Detection and imaging of nitric oxide with novel fluorescent indicators: diaminofluoresceins. *Anal Chem* **70:**2446-2453.

Kurdi M, Bowers MC, Dado J and Booz GW (2007) Parthenolide induces a distinct pattern of oxidative stress in cardiac myocytes. *Free Radic Biol Med* **42:**474-481.

Lahera V, Goicoechea M, de Vinuesa SG, Miana M, de las Heras N, Cachofeiro V and Luño J (2007) Endothelial dysfunction, oxidative stress and inflammation in atherosclerosis: beneficial effects of statins. *Curr Med Chem* **14:**243-248.

Lu YM, Shioda N, Han F, Moriguchi S, Kasahara J, Shirasaki Y, Qin ZH and Fukunaga K (2007) Imbalance between CaM kinase II and calcineurin activities impairs caffeine-induced calcium release in hypertrophic cardiomyocytes. *Biochem Pharmacol* **74:**1727-1737.

Michel JB, Feron O, Sacks D and Michel T (1997) Reciprocal regulation of endothelial nitric-oxide synthase by Ca^{2+}-calmodulin and caveolin. *J Biol Chem* **272:**15583-15586.

Michel JB, Feron O, Sase K, Prabhakar P and Michel T (1997) Caveolin versus calmodulin. Counterbalancing allosteric modulators of endothelial nitric oxide synthase. *J Biol Chem* **272:**25907-25912.

Michel T, Li GK and Busconi L (1993) Phosphorylation and subcellular translocation of endothelial nitric oxide synthase. *Proc Natl Acad Sci U S A* **90:**6252-6256.

Mollnau H, Oelze M, August M, Wendt M, Daiber A, Schulz E, Baldus S, Kleschyov AL, Materne A, Wenzel P, Hink U, Nickenig G, Fleming I and Münzel T (2005)

Mechanisms of increased vascular superoxide production in an experimental model of idiopathic dilated cardiomyopathy. *Arterioscler Thromb Vasc Bio*l **25:**2554-2559.

Mollnau H, Wendt M, Szöcs K, Lassègue B, Schulz E, Oelze M, Li H, Bodenschatz M, August M, Kleschyov AL, Tsilimingas N, Walter U, Förstermann U, Meinertz T, Griendling K and Münzel T (2002) Effects of angiotensin II infusion on the expression and function of NAD(P)H oxidase and components of nitric oxide/cGMP signaling. *Circ Res* **90:**E58-65.

Molnar J, Yu S, Mzhavia N, Pau C, Chereshnev I and Dansky HM (2005) Diabetes induces endothelial dysfunction but does not increase neointimal formation in high-fat diet fed C57BL/6J mice. *Circ Res* **96:**1178-1184.

Mount PF, Kemp BE and Power DA (2007) Regulation of endothelial and myocardial NO synthesis by multi-site eNOS phosphorylation. *J Mol Cell Cardiol* **42:**271-279.

Münzel T and Harrison DG (1999) Increased superoxide in heart failure: a biochemical baroreflex gone awry. *Circulation* **100:**216-218.

Nishino Y, Yamamoto K, Kimura S, Kikuchi A, Shiro Y and Iyanagi T (2007) Mechanistic studies on the intramolecular one-electron transfer between the two flavins in the human endothelial NOS reductase domain. *Arch Biochem Biophys* **465:**254-265.

Ostrom RS, Gregorian C, Drenan RM, Xiang Y, Regan JW and Insel PA (2001) Receptor number and caveolar co-localization determine receptor coupling efficiency to adenylyl cyclase. *J Biol Chem* **276:**42063-42069.

Ozaki M, Kawashima S, Yamashita T, Hirase T, Namiki M, Inoue N, Hirata K, Yasui H, Sakurai H, Yoshida Y, Masada M and Yokoyama M (2002) Overexpression of endothelial nitric oxide synthase accelerates atherosclerotic lesion formation in

apoE-deficient mice. *J Clin Invest* **110:**331-340.

Pou S, Pou WS, Bredt DS, Snyder SH and Rosen GM (1992) Generation of superoxide by purified brain nitric oxide synthase. *J Biol Chem* **267:**24173-24176.

Qin F, Patel R, Yan C and Liu W (2006) NADPH oxidase is involved in angiotensin II-induced apoptosis in H9C2 cardiac muscle cells: effects of apocynin. *Free Radic Biol Med* **40:**236-246.

Schulz R, Dodge KL, Lopaschuk GD and Clanachan AS (1997) Peroxynitrite impairs cardiac contractile function by decreasing cardiac efficiency. *Am J Physiol* **272:**H1212-1219.

Scriven DR, Klimek A, Asghari P, Bellve K and Moore ED (2005) Caveolin-3 is adjacent to a group of extradydic ryanodine receptor. Biophys J **89:**1893-1901

Sotgia F, Lee JK, Das K, Bedford M, Petrucci TC, Macioce P, Sargiacomo M, Bricarelli FD, Minetti C, Sudol M and Lisanti MP (2000) Caveolin-3 directly interacts with the C-terminal tail of beta -dystroglycan. Identification of a central WW-like domain within caveolin family members. *J Biol Chem* **275:**38048-38058.

Stuehr D, Pou S and Rosen GM (2001) Oxygen reduction by nitric-oxide synthases. *J Biol Chem* **276:**14533-14536.

Tachibana S, Fujimaki Y, Yokoyama H, Okazaki O and Sudo K (2005) In vitro metabolism of the calmodulin antagonist DY-9760e(3-[2-[4-(3-chloro-2-methylphenyl)-1-piperazinyl]ethyl]-5,6-dimethoxy-1-(4-imidazolylmethyl)-1H-indazole dihydrochloride 3.5 hydrate) by human liver microsomes: involvement of cytochromes p450 in atypical kinetics and potential drug interactions. *Drug Metab Dispos* **33:**1628-1636.

Takimoto E, Champion HC, Li M, Ren S, Rodriguez ER, Tavazzi B, Lazzarino G,

Paolocci N, Gabrielson KL, Wang Y and Kass DA (2005) Oxidant stress from nitric oxide synthase-3 uncoupling stimulates cardiac pathologic remodeling from chronic pressure load. *J Clin Invest* **115:**1221-1231.

Thum T, Fraccarollo D, Schultheiss M, Froese S, Galuppo P, Widder JD, Tsikas D, Ertl G and Bauersachs J (2007) Endothelial nitric oxide synthase uncoupling impairs endothelial progenitor cell mobilization and function in diabetes. *Diabetes* **56:**666-674.

Vasquez-Vivar J, Kalyanaraman B, Martasek P, Hogg N, Masters BS, Karoui H, Tordo P and Pritchard KA Jr (1998) Superoxide generation by endothelial nitric oxide synthase: the influence of cofactors. *Proc Natl Acad Sci U S A* **95**:9220-9225.

Verhaar MC, Westerweel PE, van Zonneveld AJ and Rabelink TJ (2004) Free radical production by dysfunctional eNOS. *Heart* **90:**494-495.

Waspe LE, Ordahl CP and Simpson PC (1990) The cardiac beta-myosin heavy chain isogene is induced selectively in alpha 1-adrenergic receptor-stimulated hypertrophy of cultured rat heart myocytes. *J Clin Invest* **85:**1206-1214.

Woodman SE, Park DS, Cohen AW, Cheung MW, Chandra M, Shirani J, Tang B, Jelicks LA, Kitsis RN, Christ GJ, Factor SM, Tanowitz HB and Lisanti MP (2002) Caveolin-3 knock-out mice developed a progress cardiomyopathy and show hyperactivation of the p42/44 MAPK cascade. J. Biol. Chem. **277:**38988-38997.

Xia Y, Dawson VL, Dawson TM, Snyder SH and Zweier JL (1996) Nitric oxide synthase generates superoxide and nitric oxide in arginine-depleted cells leading to peroxynitrite-mediated cellular injury. *Proc Natl Acad Sci U S A* **93:**6770-6774.

Xia Y, Tsai AL, Berka V and Zweier JL (1998) Superoxide generation from endothelial nitric-oxide synthase. A Ca^{2+}/calmodulin-dependent and tetrahydrobiopterin

regulatory process. *J Biol Chem* **273:**25804-25808.

Xiao L, Pimentel DR, Wang J, Singh K, Colucci WS and Sawyer DB (2002) Role of reactive oxygen species and NAD(P)H oxidase in alpha(1)-adrenoceptor signaling in adult rat cardiac myocytes. *Am J Physiol Cell Physiol* **282:**C926-934.

Xu KY, Huso DL, Dawson TM, Bredt DS and Becker LC (1999) Nitric oxide synthase in cardiac sarcoplasmic reticulum. *Proc Natl Acad Sci U S A* **96:**657-662.

Yasmin W, Strynadka KD and Schulz R (1997) Generation of peroxynitrite contributes to ischemia-reperfusion injury in isolated rat hearts. *Cardiovasc Res* **33:**422-432.

Zou MH, Shi C and Cohen RA (2002) Oxidation of the zinc-thiolate complex and uncoupling of endothelial nitric oxide synthase by peroxynitrite. *J Clin Invest* **109:**817-826.

Footnote:

This work was supported in part by grants-in-aid for Scientific Research from the Ministry of Education, Science, Sports and Culture of Japan (19390150 to K.F.) and the Smoking Research Foundation (to K.F.).

Molecular Pharmacology Fast Forward. Published on October 24, 2008 as DOI: 10.1124/mol.108.050716
This article has not been copyedited and formatted. The final version may differ from this version.

Figure Legends

Figure 1. Temporal changes in expression of eNOS and caveolin-3 in total homogenates, and membrane and cytosol fractions after phenylephrine (PE) treatment of rat cultured cardiomyocytes. (A) (upper) Representative image of an immunoblot probed with an anti-eNOS antibody. Changes in amounts of 135 kDa eNOS in total homogenates (total), and membrane and cytosolic fractions were seen after PE (10 μM) treatment for the indicated times. (lower) Quantitation of eNOS levels was performed by densitometry. **(B)** (upper) Representative image of immunoblot probed with anti-caveolin-3 (Cav-3) antibody. (lower) Quantitation of 18-kDa caveolin-3 levels was analyzed by densitometry. Data are means ± SEM of 3 independent experiments performed in triplicate. $^{*}P<0.05$; $^{**}P<0.01$ vs. control cells; $^{\#}P<0.05$; $^{\#\#}P<0.01$ vs. 48 h.

Figure 2. Ca^{2+}-dependent production of NO after prolonged PE treatment. (A) Changes in DAF fluorescence after treatment with A23187 (0.5 μM) in the presence or absence of DY-9836 (5 or 10 μM). NO production in cultured cardiomyocytes was assessed with the NO-sensitive fluorescence probe DAF without treatment (Control; Con), or at 48 and 96 h of PE treatment. DAF fluorescence intensity was monitored at excitation and emission wavelengths of 488 nm and 520 nm, respectively. Marked NO elevation following A23187 stimulation at 48 h was dose-dependently inhibited by pretreatment with DY-9836 (5 and 10 μM). **(B)** Quantitation of changes in DAF fluorescence intensity with or without A23187 stimulation in control or at 48 and 96 h of PE treatment. Fluorescence intensity of untreated control cells was defined as 100%. Data are means ± SEM of 3 independent experiments performed in triplicate. $^{*}P<0.05$;

Molecular Pharmacology Fast Forward. Published on October 24, 2008 as DOI: 10.1124/mol.108.050716
This article has not been copyedited and formatted. The final version may differ from this version.

$^{**}P<0.01$; $^{***}P<0.001$ vs. control cells; $^{\#\#}P<0.01$ vs. 48 h.

Figure 3. **Changes in basal $O_2^{\cdot-}$ generation after prolonged PE treatment. (A)** Representative image of DHE fluorescence with or without PE treatment. $O_2^{\cdot-}$ production in cultured cardiomyocytes was monitored using the oxidative fluorescent dye DHE before (Control; Con) or after PE treatment (PE 48 or 96 h) in the presence or absence of A23187, L-NAME and/or apocynin. Basal $O_2^{\cdot-}$ fluorescence was approximately 300 arbitrary units. Basal $O_2^{\cdot-}$ fluorescence was markedly elevated to approximately 600 at 96 h of PE treatment. Elevated $O_2^{\cdot-}$ fluorescence is reduced by apocynin treatment and further inhibited by L-NAME treatment, as shown in the panel (c). Aberrant $O_2^{\cdot-}$ elevation was also inhibited by DY-9836 dose-dependently as seen in panel (d). **(B)** Quantitation of changes in DHE fluorescence intensity with or without various treatments in control cells and in 48 or 96 h PE-treated cells. Data are expressed as percentage of values versus PE-untreated cells (control) to exclude potential culture media affects. (means ± SEM). $^{*}P<0.05$; $^{**}P<0.01$ vs. PE-untreated cells cells; $^{\#\#}P<0.01$ vs. 96 h. **(C)** Changes in eNOS dimer/monomer ratio after PE exposure. Immunoblot analysis of low-temperature SDS-PAGE revealed two bands for eNOS protein in extracts from PE-treated cardiomyocytes, representing a 130-kDa eNOS monomer and a 250-kDa eNOS dimer. $^{**}P<0.01$; $^{***}P<0.001$ vs. control cells, $^{\#\#}P<0.01$ vs. 48 h.

Figure 4. **Effects of prolonged DY-9836 treatment on NO and O_2^{-} production in PE-treated cardiomyocytes. (A)** DY-9836 (1 and 3μM) with or without L-NAME (100 μM) was added in culture medium after 48 h of PE treatment. At 96 h, NO levels were measured by DAF fluorescence. Prolonged DY-9836 (1 to 3 μM) treatment

Molecular Pharmacology Fast Forward. Published on October 24, 2008 as DOI: 10.1124/mol.108.050716
This article has not been copyedited and formatted. The final version may differ from this version.

dose-dependently inhibited elevated NO levels in PE-treated cells. L-NAME (100 μM) completely suppressed NO levels to control levels. Fluorescence intensity of untreated control cells is expressed as 100%. **(B)** DY-9836 (1 and 3μM) and L-NAME (100 μM) with or without Tempol (1 mM) were added to culture medium after 48 h of PE treatment. Prolonged DY-9836 (1 to 3 μM) treatment dose-dependently suppressed $O_2^{\cdot-}$ generation. TEMPOL (1 mM) totally suppressed $O_2^{\cdot-}$ generation in PE-treated cells. Data are expressed as percentage of values versus PE-untreated cells to exclude media effects. Data are means ± SEM of 3 independent experiments performed in triplicate. $^{**}P<0.01$ vs. control cells; $^{\#\#}P<0.01$ vs. 96 h.

Figure 5. **Effects of DY-9836 treatment on dystrophin/caveolin-3 breakdown and eNOS uncoupling. (A)** Effect of DY-9836 on dystrophin breakdown in cultured cardiomyocytes. After 48 h exposure to PE, DY-9836 (1 or 3 μM) was added to culture medium and further incubated with PE for another 48 h. Membrane extracts were prepared from control cells and from 48 or 96 h PE-treated cells and subjected to immunoblotting with anti-dystrophin antibody. Elevated dystrophin underwent significant breakdown at 96 h. DY-9836 (3 μM) treatment for the last 48 h significantly inhibited dystrophin breakdown. $^{*}P<0.05$; $^{**}P<0.01$ vs. control cells, $^{\#\#}P<0.01$ vs. 48 h; $^{\S\S}P<0.01$ vs. 96 h. **(B)** Effect of DY-9836 on caveolin-3 breakdown. Membrane extracts were prepared from control cells and from 96 h PE-treated cells and immunoblotted with anti-caveolin-3 antibody. DY-9836 (1 and 3 μM) treatment for the last 48 h significantly inhibited caveolin-3 breakdown dose-dependently. $^{*}P<0.05$; $^{**}P<0.01$ vs. control cells, $^{\#\#}P<0.01$ vs. 96 h. **(C)** Effect of DY-9836 on eNOS uncoupling observed at 96 h of PE treatment. Total cell extracts were prepared from control cells or PE-treated

Molecular Pharmacology Fast Forward. Published on October 24, 2008 as DOI: 10.1124/mol.108.050716
This article has not been copyedited and formatted. The final version may differ from this version.

cells. Dimeric and monomeric forms of eNOS were assessed by low-temperature SDS-PAGE. Quantitation of dimeric and monomeric eNOS was performed by densitometric analysis, and the dimer/monomer ratio relative to controls is represented by the bar graph. The dimer/monomer ratio in control cells was expressed as 1. **P<0.01 vs. control cells. $^{\#}$P<0.05, $^{\#\#}$P< 0.01 vs. 96 h. Data are means ± SEM of 3 independent experiments performed in triplicate.

Figure 6. **Inhibition of PE-induced cardiomyocyte apoptosis by DY-9836 treatment.** **(A)** Cells were treated with PE (10 μM) for 48 h and 96 h. DY-9836 (3 μM), L-NAME (100 μM) and TEMPOL (1 mM) were added to the culture medium during the last 48 h. Detection of apoptosis was by TUNEL staining (green). Panels a; control, b; PE48h, c; PE 96h, d; TEMPOL (1 mM) + PE 96h. e; DY-9836 (3 μM)+ PE 96h, f; L-NAME (100 μM)+ PE 96h **(B)** The percentage of TUNEL-positive nuclei was calculated by ratio of TUNEL-positive cells shown in panel A to the total cell numbers. Pooled data from 3 independent experiments are presented as means ± SEM (n = 100). *P<0.05; **P<0.01 vs. control; $^{\#\#}$P<0.01 vs. 96 h.

Figure 7

Immunocytochemical localization of caveolin-3 and eNOS after PE treatment with or without DY-9836 treatment. After 24 h of culture with serum-free DMEM, cells were treated with PE (10 μM) for 48 or 96 h in the presence or absence of DY-9836 (3 μM), L-NAME (100 μM) and TEMPOL (1 mM) **(A)** Confocal microscopic images of cells double stained with anti-caveolin-3 (red) and anti-eNOS (green) antibodies, indicating predominant expression of caveolin-3 (a) and eNOS (b) in membranous or

cytoskeletal elements in control and PE-treated cardiomyocytes. Markedly decreased caveolin-3 (g) and eNOS (h) immunofluorescence was observed in cardiomyocytes after 96 h of PE treatment. Dissociation of caveolin-3 (j) and eNOS (k) from the membrane was blocked by DY-9836 treatment. Scale bar=30 μm. Panels a, b, c from control cells (Con); d, e, f from PE(48h)-exposed cells; g, h, I from PE(96h) exposed cells; j, k, l from DY-9836 (3μM) + PE(96h)-exposed cells **(B)** Cells were fixed with 4% paraformaldehyde, stained with a monoclonal antibody against rhodamine-phalloidin, and processed for microscopy. Morphological alteration of cardiomyocytes assessed by rhodamine-phalloidin staining was observed after PE treatment. PE (48h) and PE (96h)-exposed cells show enlargement of cell size and DY-9836 treatment inhibited the enlargement of cell size by PE treatment. Scale bar=20μm. **(C)** Cell size results are expressed as relative surface area standardized to the mean surface area of control cells in each experiment. Pooled data from 3 independent experiments are presented as means ± SEM (n = 100). $^{**}P < 0.01$ vs. control; $^{\#\#}P < 0.01$ vs. 96 h.

Figure 8

Possible mechanism of NO and superoxide production by coupled and uncoupled eNOS, respectively. eNOS, a dimeric, bidomain enzyme consisting of a C-terminal functionally reductase domain which binds NADPH, flavin, FAD and FMN, as well as a N-terminal functionally oxygenase domain, where haem, BH4 and L-arginine bind. The two domains are linked each other by a calmodulin-binding site. The eNOS cofactor tetrahydrobiopterin (BH4) facilitates the reaction of electrons and oxygen with L-arginine leading to the formation of L-citrulline and NO. Lack of BH4 by its oxidation induces disruption of the superoxy ferrous–peroxy ferric complex. However,

Molecular Pharmacology Fast Forward. Published on October 24, 2008 as DOI: 10.1124/mol.108.050716
This article has not been copyedited and formatted. The final version may differ from this version.

electrons (e-) are still donated by NADPH to the reductase domain of eNOS monomer, and in turn donate the electrons one-at-a-time to O_2 in the oxygenase domain, resulting in a one electron reduction to form superoxide (modified from Förstermann and Münzel, 2006).

Figure 9

Possible mechanism of PE-induced oxidative injury by eNOS uncoupling and sites of DY-9836 action. In the compensatory phase of PE-induced hypertrophy, eNOS induction triggers elevated Ca^{2+}-induced NO production, which is cardioprotective because of inhibition of Ca^{2+} elevation by PE stimulation. Elevation of caveolin-3 and dystrophin levels in the membrane fraction is a compensatory phenomenon in PE-induced hypertrophic cardiomyocytes. However, further exposure to PE (96 h) (decompensatory phase) initiates caveolin-3/dystrophin breakdown with concomitant eNOS uncoupling by oxidative stress. Lack of caveolin-3/dystrophin in caveolae also promotes eNOS dissociation from caveolae. Cardioprotective effects of DY-9836 are likely mediated by inhibiting caveolin-3/dystrophin breakdown and inhibiting NO and $O_2^{\cdot-}$ production by coupled and uncoupled eNOS, respectively. Dys, dystrophin; Cav-3, caveolin-3; CaM, calmodulin; $ONOO^-$, peroxynitrite.

Molecular Pharmacology Fast Forward. Published on October 24, 2008 as DOI: 10.1124/mol.108.050716
This article has not been copyedited and formatted. The final version may differ from this version.

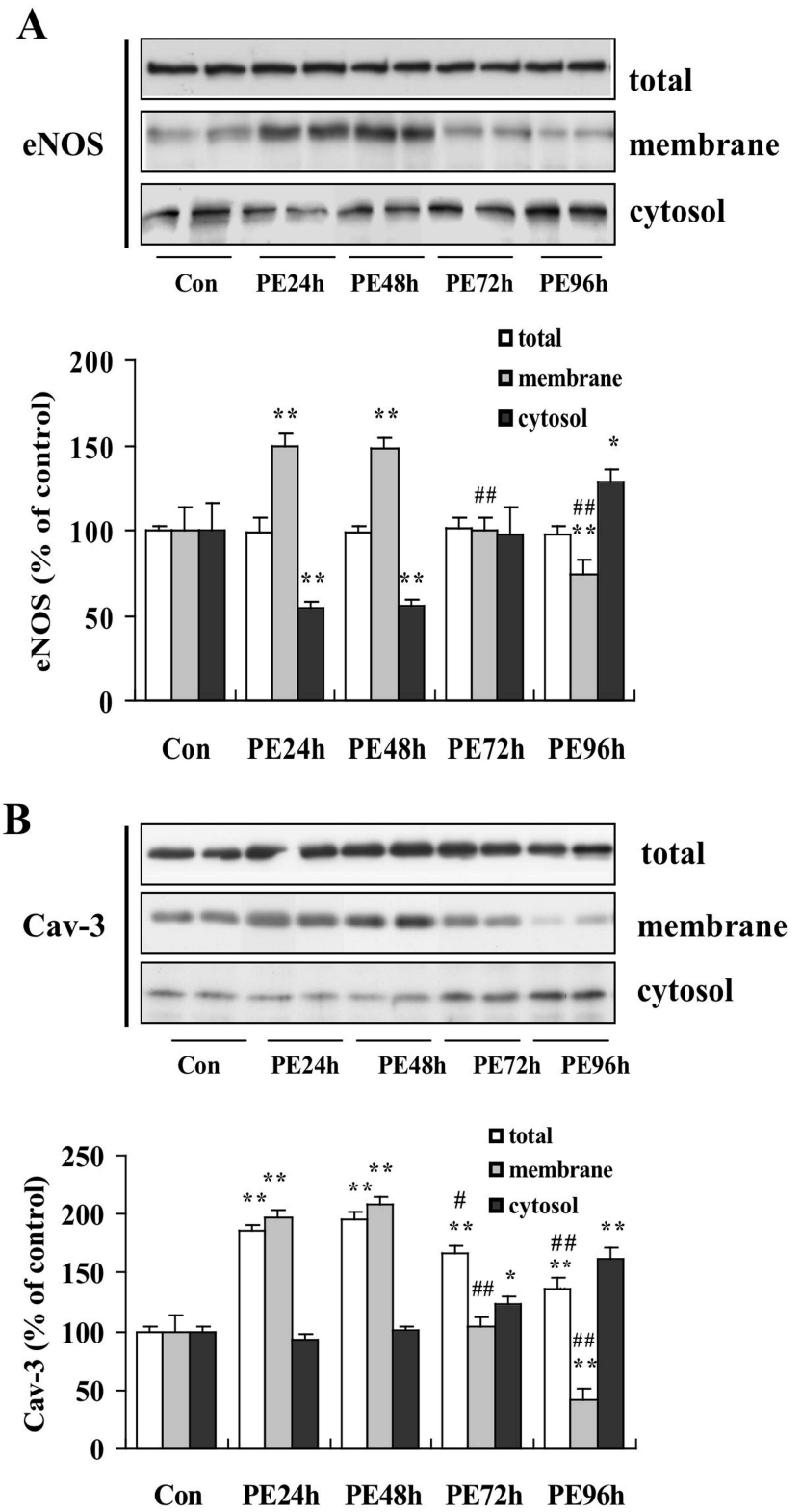

Fig. 1

Molecular Pharmacology Fast Forward. Published on October 24, 2008 as DOI: 10.1124/mol.108.050716
This article has not been copyedited and formatted. The final version may differ from this version.

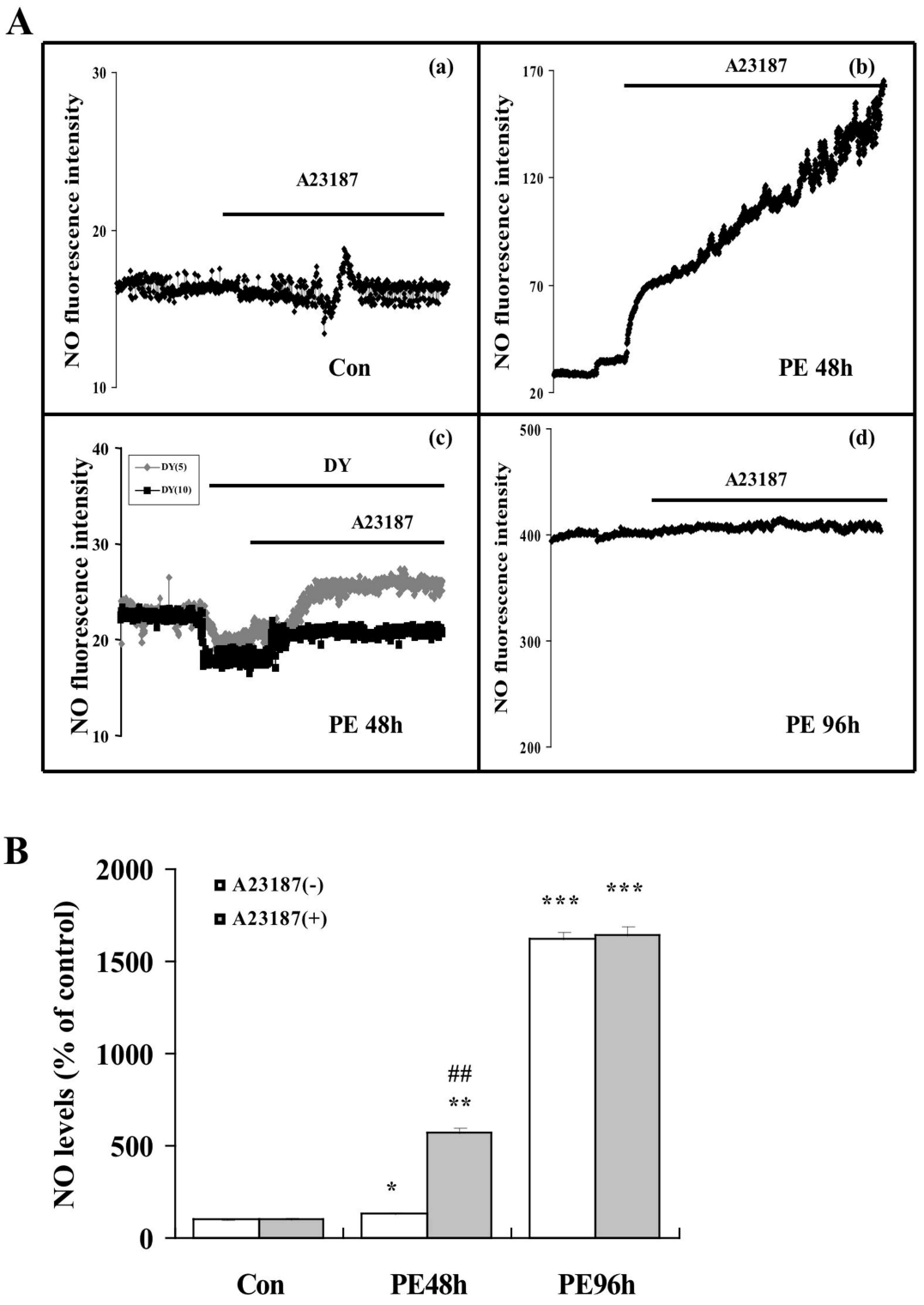

Fig. 2

Molecular Pharmacology Fast Forward. Published on October 24, 2008 as DOI: 10.1124/mol.108.050716
This article has not been copyedited and formatted. The final version may differ from this version.

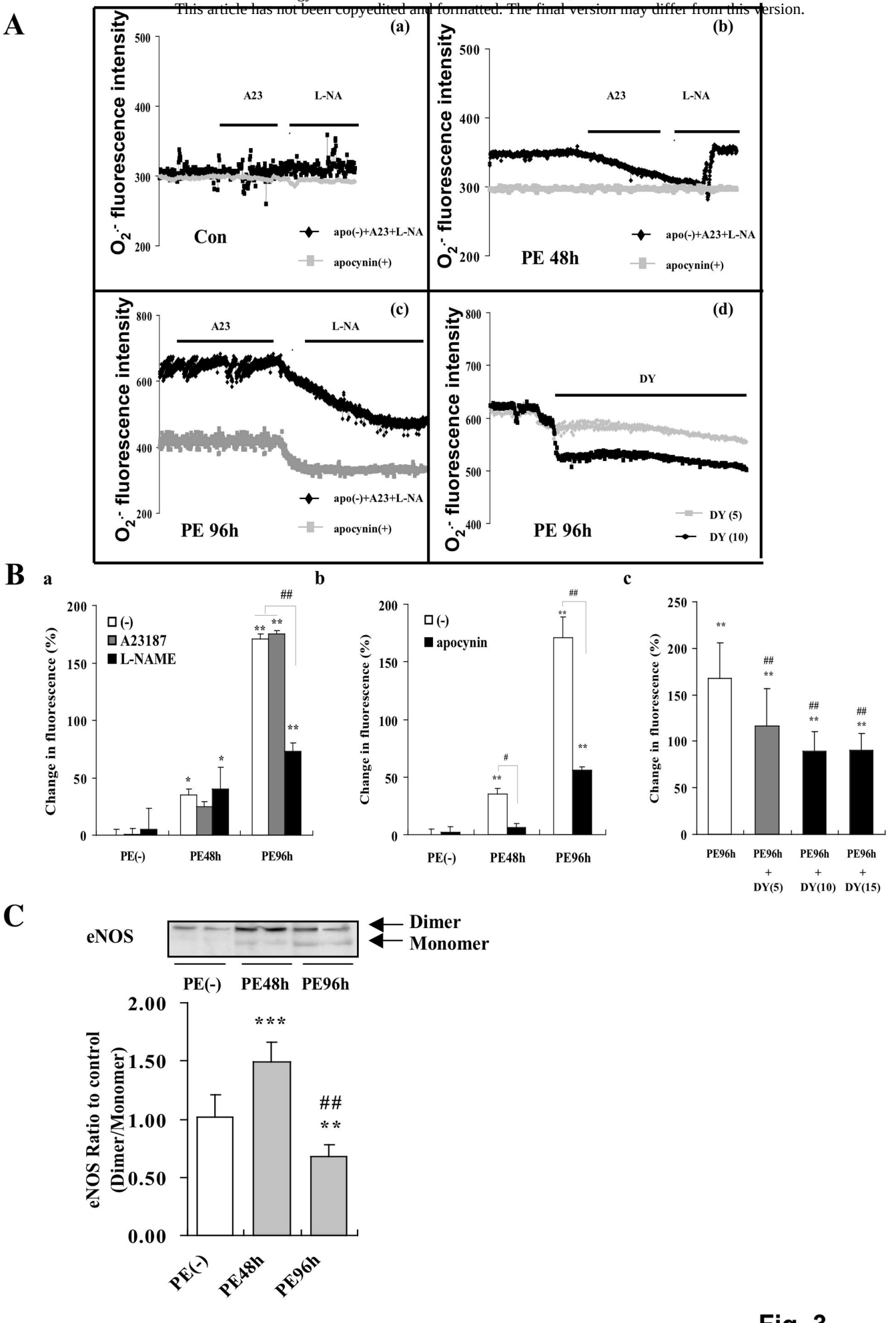

Fig. 3

Molecular Pharmacology Fast Forward. Published on October 24, 2008 as DOI: 10.1124/mol.108.050716
This article has not been copyedited and formatted. The final version may differ from this version.

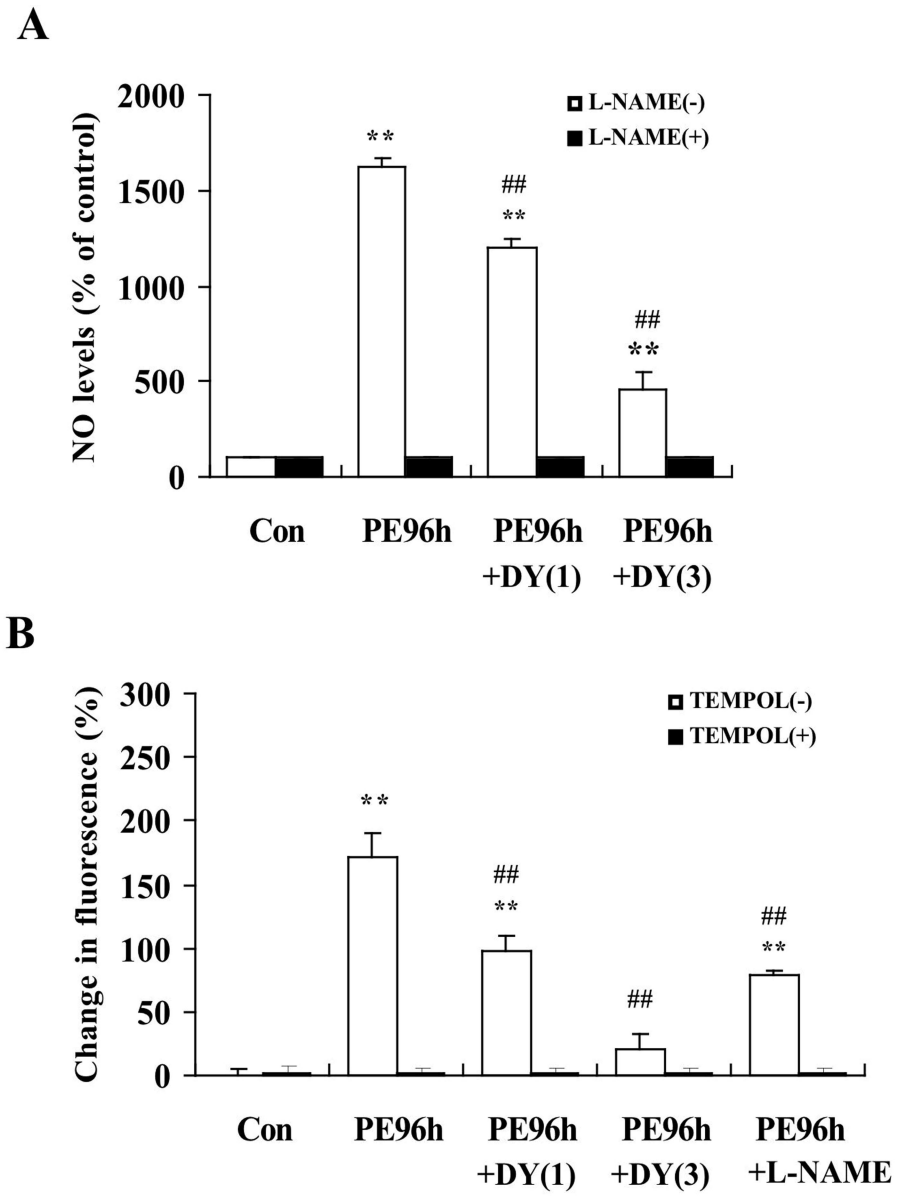

Fig.4

Molecular Pharmacology Fast Forward. Published on October 24, 2008 as DOI: 10.1124/mol.108.050716
This article has not been copyedited and formatted. The final version may differ from this version.

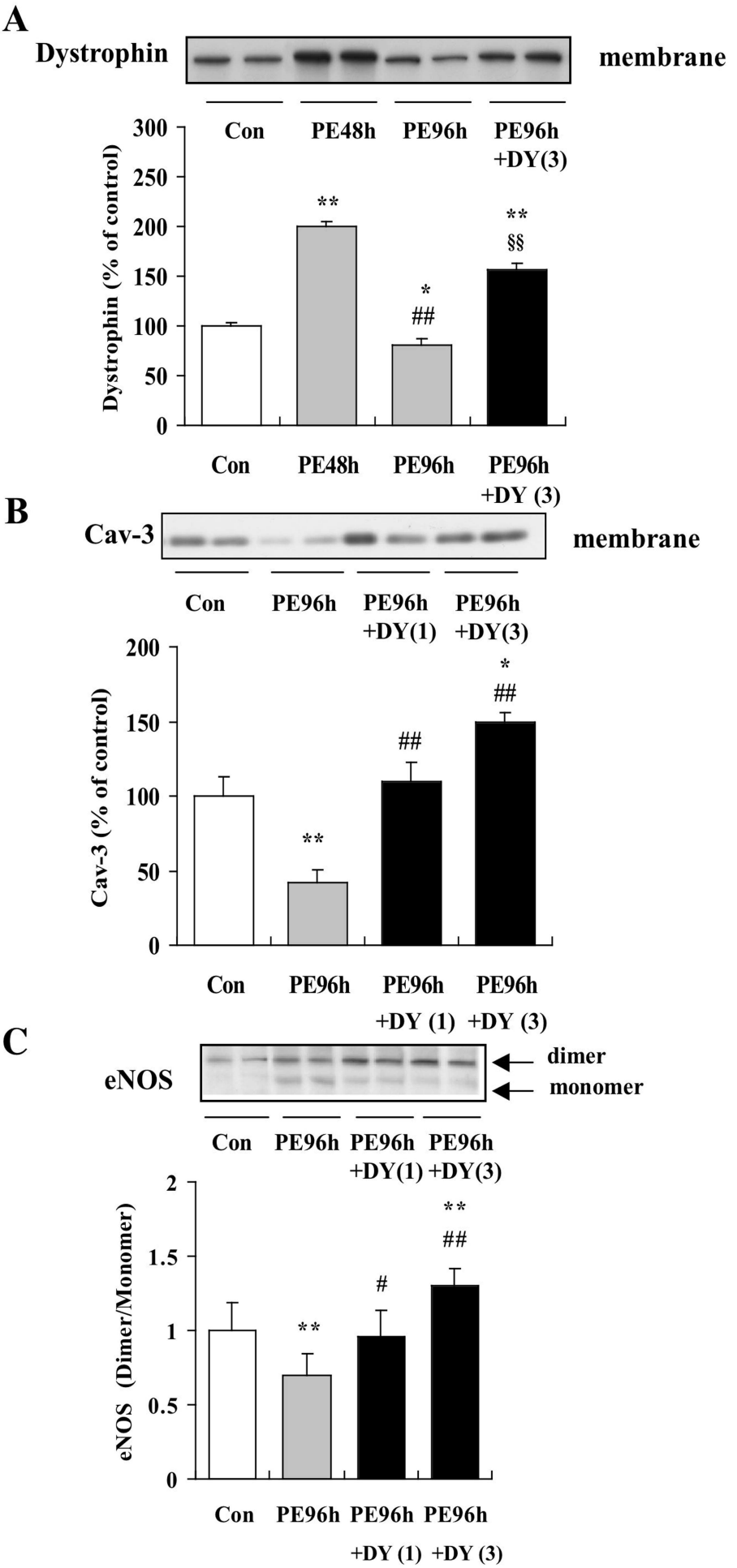

Fig. 5

Molecular Pharmacology Fast Forward. Published on October 24, 2008 as DOI: 10.1124/mol.108.050716
This article has not been copyedited and formatted. The final version may differ from this version.

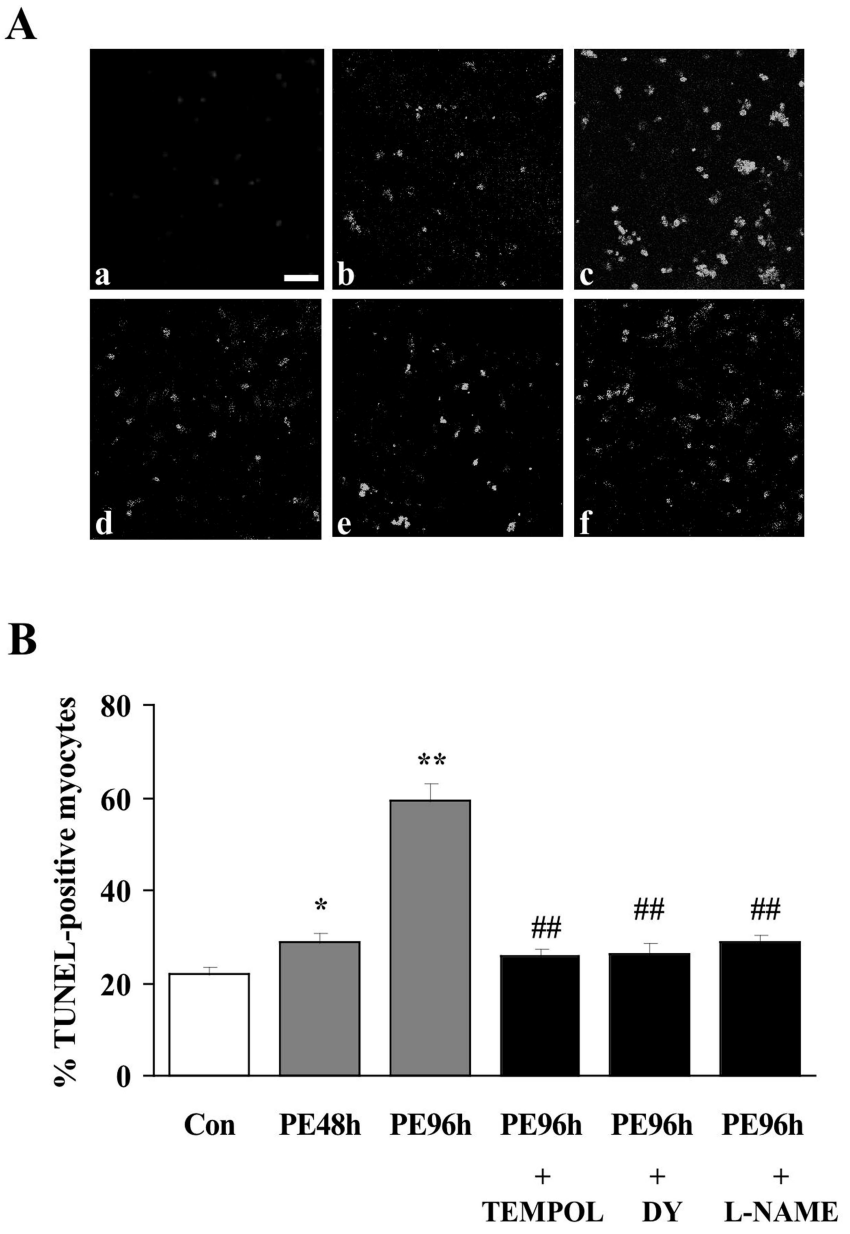

Fig. 6

Molecular Pharmacology Fast Forward. Published on October 24, 2008 as DOI: 10.1124/mol.108.050716
This article has not been copyedited and formatted. The final version may differ from this version.

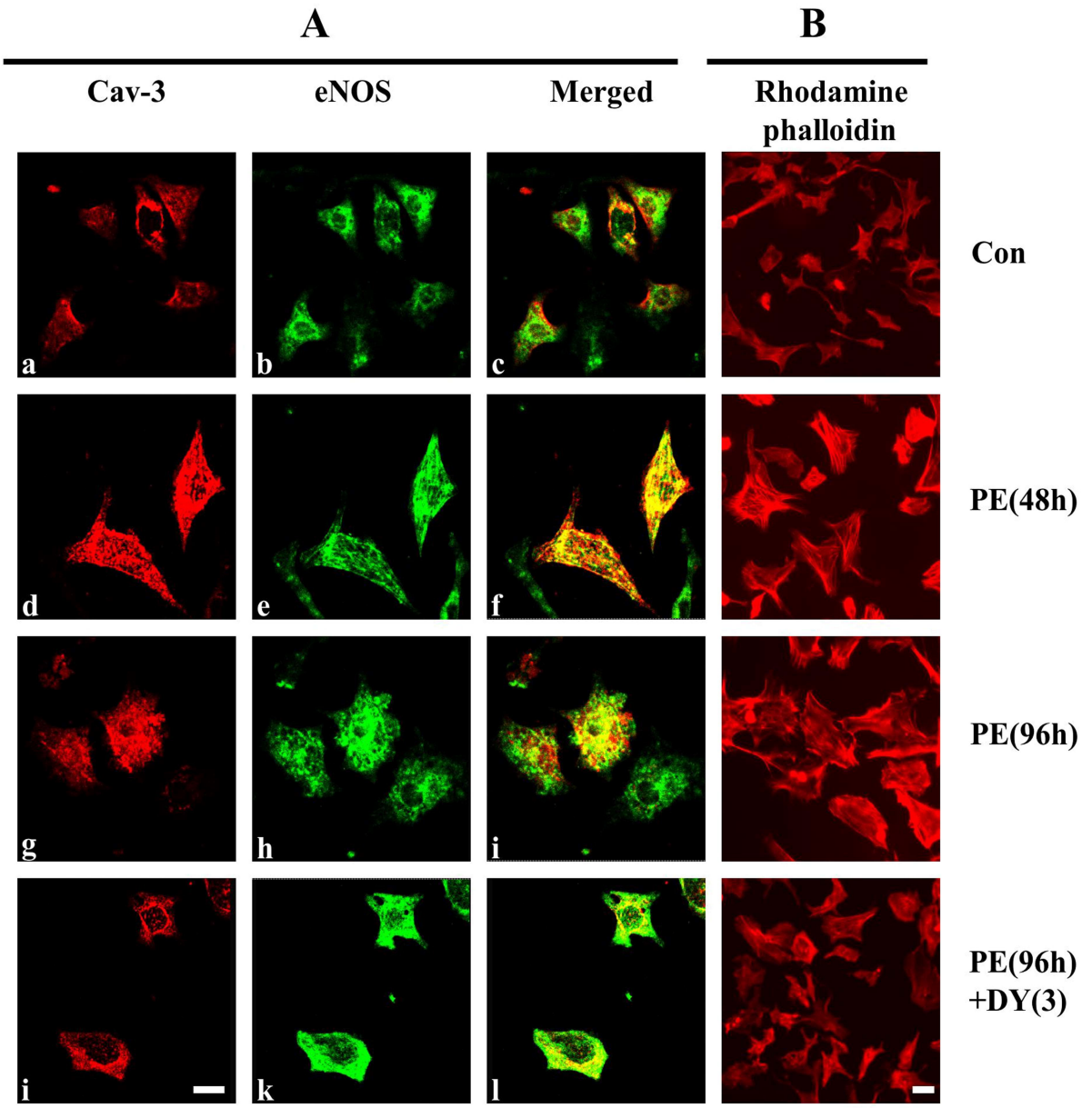

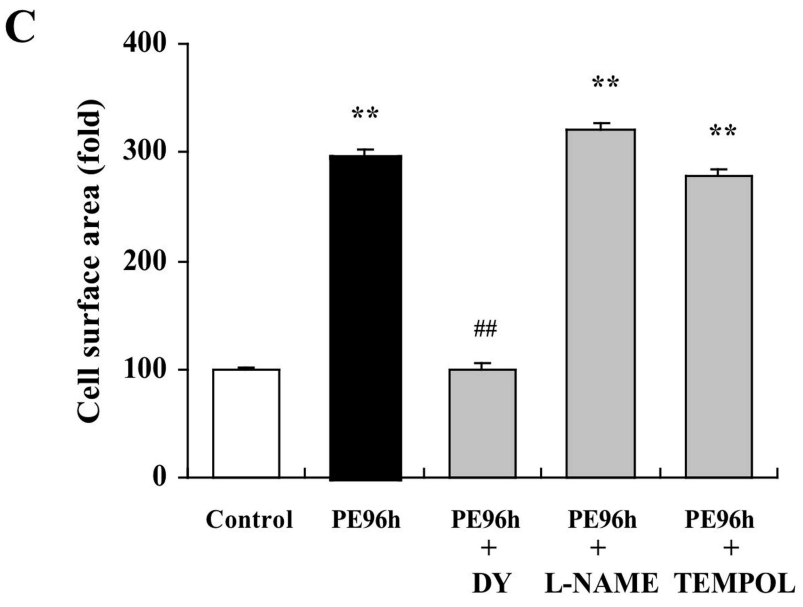

Fig. 7

Molecular Pharmacology Fast Forward. Published on October 24, 2008 as DOI: 10.1124/mol.108.050716
This article has not been copyedited and formatted. The final version may differ from this version.

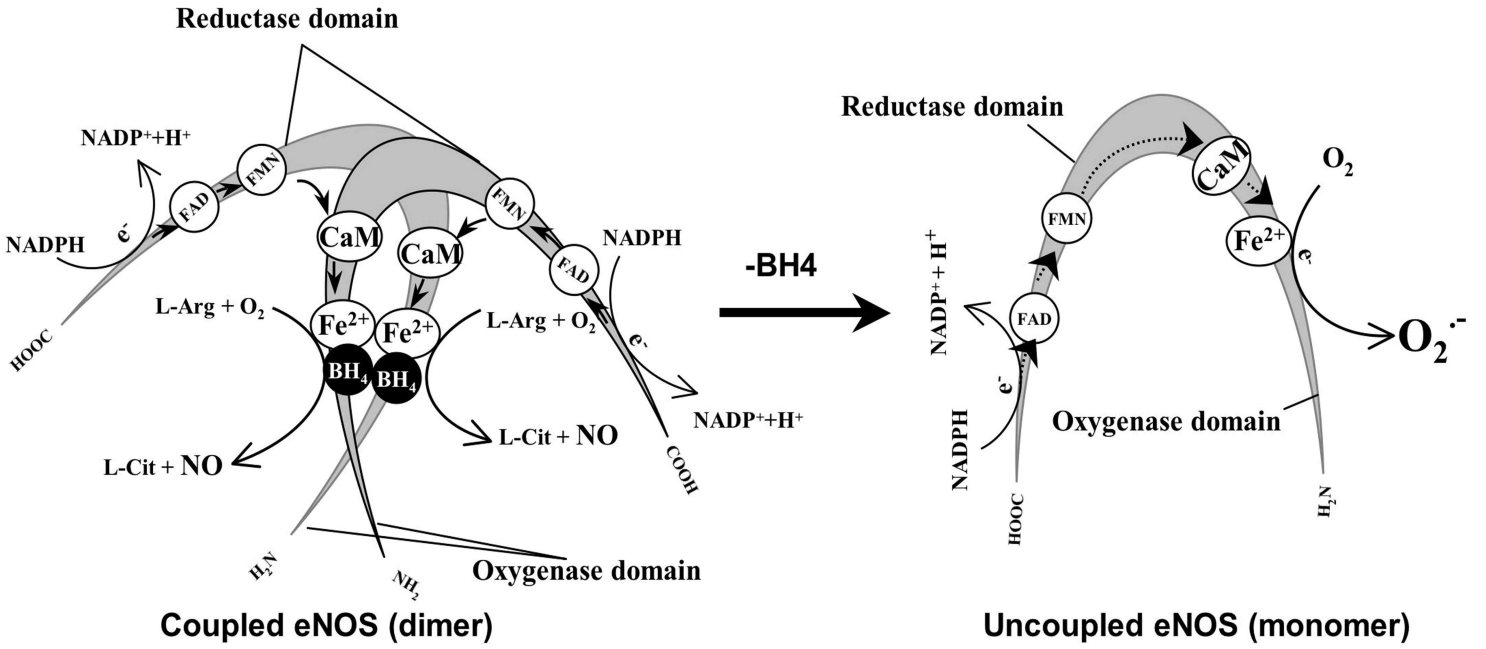

Fig. 8

Molecular Pharmacology Fast Forward. Published on October 24, 2008 as DOI: 10.1124/mol.108.050716
This article has not been copyedited and formatted. The final version may differ from this version.

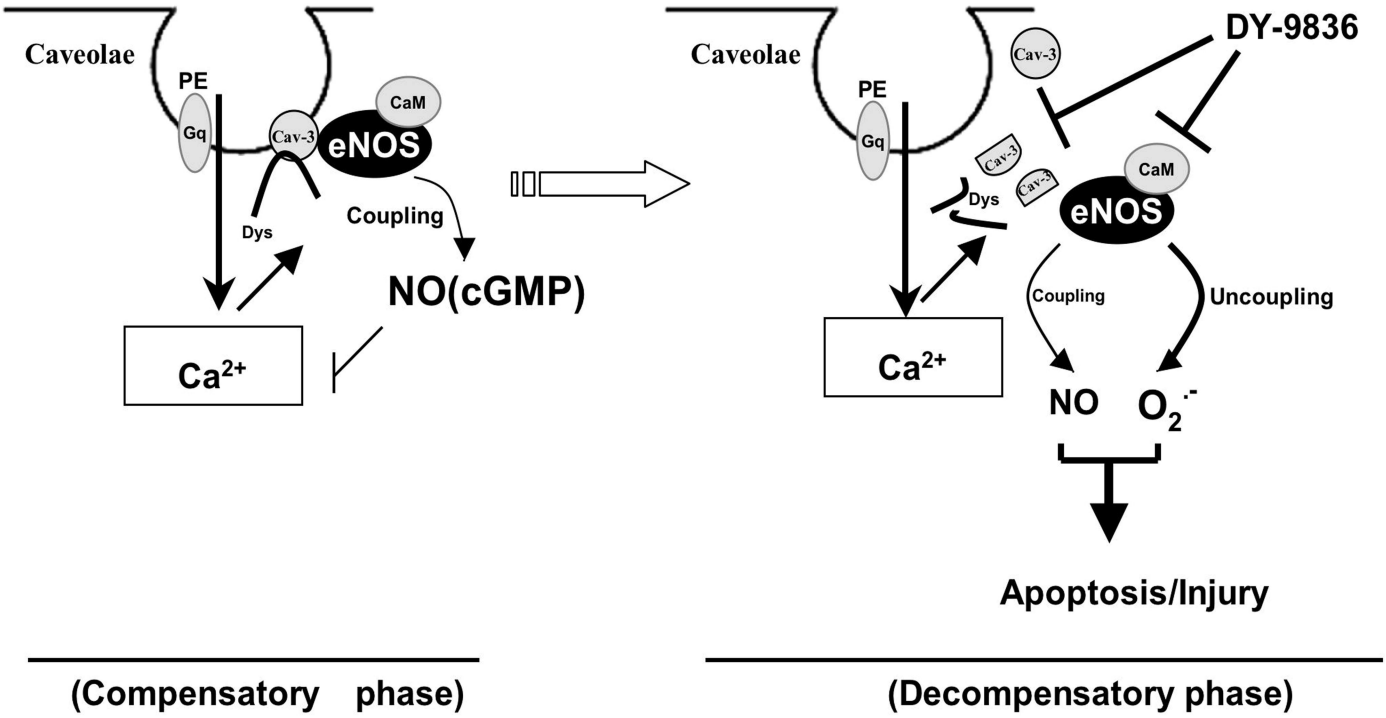

Fig. 9